The Impact of Satellite Winds and Latent Heat Fluxes in a Numerical Simulation of the Tropical Pacific Ocean

LUDOS-HERVE AYINA AND ABDERRAHIM BENTAMY

Laboratoire d'Océanographie Spatiale (DOPS/LOS), IFREMER, Plouzané, France

ALBERTO M. MESTAS-NUÑEZ

Cooperative Institute for Marine and Atmospheric Studies, University of Miami, Miami, Florida

GURVAN MADEC

Laboratoire d'Océanographie et du Climat-Expérimentation et Analyse Numérique (LOCEAN), Paris, France

ABSTRACT

Several oceanic operational programs use remotely sensed fluxes to complement atmospheric operational analyses from major national weather prediction centers. The main goal of this study is to evaluate the ability of the ocean model (ORCA) to correctly simulate the dynamic of the tropical Pacific Ocean in 1996–98 when forced by the satellite turbulent fluxes (wind stress and latent heat fluxes). The results are compared with the oceanic response resulting from forcing the model with the European Centre for Medium-Range Weather Forecasts (ECMWF) operational analysis. Three sensitivity simulations forced with satellite and atmospheric analysis fields are performed. The control experiment is forced with the ECMWF fluxes. The solutions of these simulations are compared with data from the Tropical Atmosphere–Ocean (TAO) buoys and from sea surface temperatures analysis by Reynolds and Smith in the equatorial Pacific Ocean. The analysis results indicate that the model reproduces well the major spatial and temporal oceanic structures including the main characteristics of the 1997–98 El Niño. More specifically, the comparisons with buoys indicate that the experiment forced by the winds and the satellite latent heat fluxes is closer to the observations. They provide weak rms difference and strong correlations along the whole 500-m depth column. Furthermore, the correlations with the SST analysis vary between 75% and 95% compared to 65% and 77% for the experiment forced by ECMWF fluxes. The currents in the first 350 m also show a strong sensitivity to satellite turbulent fluxes.

1. Introduction

One of the tasks of operational oceanography is to use a numerical model to simulate and forecast the oceanic general circulation on various spatial and temporal scales. The modeling of the oceanic circulation requires accurate knowledge of the turbulent fluxes exchanged at the ocean–atmosphere interface. The main surface fluxes involved in this exchange are the momentum flux (wind stress), the turbulent heat fluxes (latent and sensible), and the freshwater fluxes (evaporation and precipitation). Operational oceanic programs like the European Mercator Océan (www.mercator-ocean.fr), Mediterranean Forecast System Toward Environmental Predictions (MFSTEP) (www.bo.ingv.it/mfstep), and Marine Environment and Security for the European Area (MERSEA; www.mersea.eu.org) routinely use forcing fields from the European Centre for Medium-Range Weather Forecasts (ECMWF) operational analysis. These fluxes generally have good temporal resolution but poor spatial resolution (about 250 km). Therefore, they do not accurately represent small-scale phenomena (mesoscales), which have a space resolution of about 25 to 100 km. The operational oceanic programs, mentioned above, consider that the remotely sensed fluxes should be used as complementary and/or alternative data sources to the ECMWF forcing func-

Corresponding author address: Ludos-Herve Ayina, Laboratoire d'Océanographie Spatiale (DOPS/LOS), IFREMER, B.P. 70, 29280 Plouzané, France.
E-mail: lhayina@ifremer.fr

tion. Actually, the sampling of the satellite data allows enhancing the spatial resolution of surface fluxes over the global ocean. However, before using the satellite data in operational forcing experiments, it is necessary to characterize the oceanic response to the forcing function determined from satellite data, in order to understand their advantages and disadvantages.

Several studies have analyzed the quality of the satellite turbulent fluxes through comparisons with fluxes resulting from meteorological analyses/reanalyses or with in situ data (Bentamy et al. 1999, 2003). Other studies have been devoted to their impact on the oceanic circulation (Grima et al. 1999; Blanke et al. 2002, 2005). For example, using a Pacific tropical model forced with *European Remote Sensing Satellite-1/-2* (*ERS-1/-2*) wind stress, Grima et al. (1999) showed a significant contribution of these winds to the circulation in this region. In addition, Vialard et al. (2001) were able to describe the major structures of El Niño (1997–98) using ERS1/2 winds stress. The recent work of Blanke et al. (2005), which associates the Quick Scatterometer (QuikSCAT) winds stress and the interannual variability of SST in the Benguela upwelling region, suggests a high impact of these satellite winds in that particular dynamic system.

The analyses mentioned above and others have demonstrated the usefulness of satellite turbulent fluxes in oceanic simulations focusing mainly on the impact of satellite winds. The present study, however, focuses on the impact of satellite latent heat fluxes (LHFs) on ocean simulations. We investigate the quality of the satellite latent heat fluxes by using them in combination with scatterometer wind stresses to force an oceanic general circulation model. Even though the oceanic model used here is global, we base our study on the response of the tropical Pacific Ocean during the 3-yr period 1996–98. During this period, validated winds and latent heat fluxes are available globally with equal space and time resolution. This period includes large climatic variability in the tropical Pacific due to the very strong 1997–98 El Niño, which was followed by the strong 1998–99 La Niña (Wang and McPhaden 2001; Vialard et al. 2001; Picaut et al. 2002; Mestas-Nuñez et al. 2006). The tropical Atmosphere–Ocean (TAO) buoy network allows us to assess the quality of the simulations through comparisons between the oceanic model results and the buoy measurements.

The organization of this paper is as follows: in section 2, we present the satellite turbulent fluxes, the oceanic general circulation model (OGCM), the sensitivity experiments, and the observations used to evaluate the quality of the simulations. The response of the Pacific Ocean in the various sensitivity simulations is compared and discussed in section 3. We summarize our conclusions in section 4.

2. Data and model

a. Forcing data

The remotely sensed winds and latent heat fluxes are mainly derived from the scatterometers on board the *ERS-1* and *ERS-2* and from the radiometers on board the Defense Meteorological Satellite Program (DMSP; *F10* and *F11*). The methods used to derive the satellite turbulent fluxes are described in Bentamy et al. (2003). They are based on the bulk aerodynamic formulas that parameterize the wind stress and latent heat flux:

$$\tau = (\tau_x, \tau_y) = \rho C_{\mathrm{Dn}} \overline{U}_{10n}(u_{10n}, v_{10n}) \qquad (1)$$

$$Q_{\mathrm{latent}} = -l\rho C_{\mathrm{En}} \overline{U}_{10n}(q_{a_{10n}} - q_s), \qquad (2)$$

where τ is the wind stress vector and τ_x, τ_y are its zonal and meridional components, respectively. Here, Q_{latent} is the latent heat flux; $\overline{U}_{10n}(u_{10n}, v_{10n})$ is the surface wind speed (zonal and meridional components); q_s and q_{a10n} are the specific humidity at the sea surface equivalent to the saturation value at the sea surface temperature and the air specific humidity at 10-m height, respectively, in kg kg^{-1}; l is the latent heat of evaporation in J kg^{-1}; ρ is the air density (kg m^{-3}); and C_{Dn} and C_{En} are the bulk drag and the transfer coefficient for water vapor, respectively. The subscript (n) refers to neutral stability conditions. The transfer coefficients (C_{Dn} and C_{En}) are estimated using the Smith (1988) algorithm in the neutral stability conditions, and they are both functions of the surface wind speed (U_{10n}) (Bentamy et al. 2003). The input variables $\overline{U}_{10n}$, q_{a10n}, and sea surface temperature (SST), from which q_s is calculated, are estimated from satellite observations (e.g., Bentamy et al. 2002a, 2003; Liu and Niiler 1984; Schulz et al. 1993, 1997).

The study concentrated on the period when several satellite wind data were available over the global ocean. During the period January 1996 through December 1998, the *ERS-1/-2* satellites obtained a single 500-km swath of wind vectors at 50-km resolution, and several Special Sensor Microwave Imagers (SSM/Is) on board *F10* and *F11* DMSP satellites provided wind speeds over 1400-km swaths. The latter provide near-surface humidity too. The missing ingredient, SST, was obtained from the Reynolds and Smith analysis (Reynolds and Smith 1994).

The quality of the derived surface winds and latent heat fluxes was investigated through comprehensive comparisons with buoy and ship estimates (Bentamy et

TABLE 1. Mean values of the wind stress amplitude and LHF from ECMWF. The bias characterizing the comparisons between ECMWF and satellite products SAT; (wind stress and LHF), and between ECMWF and the New ECMWF (NECMWF; wind stress) in the entire, western (160°E–180°), central (170°–140°W), and eastern (130°–110°W) Pacific, between 5°S and 5°N. The NECMWF refers to the daily fields interpolated from the weekly average. The units of wind stress and LHF are 10^{-2} and W m^{-2}, respectively.

Mean/bias	Global	West	Central	East
Mean wind stress (ECMWF)	5.2	5.0	6.0	4.5
SAT − ECMWF	−0.8	−0.8	−0.9	−0.7
NECMWF − ECMWF	−0.08	−0.1	−0.08	−0.07
Mean LHF (ECMWF)	−152	−162	−156	−132
SAT − ECMWF	−23	−21	−27	−24

al. 2002a, 2003). The remotely sensed flux observations are then used to estimate regular flux fields in space and time over the global ocean.

The present study employs the weekly averaged fluxes at $1° \times 1°$ resolution available during the study period 1996–98. The accuracy of the resulting weekly fields is determined by comparisons with moored-buoy wind and latent heat flux estimates, which are deployed and maintained by four different institutions in the Atlantic and Pacific Oceans. The agreement between satellite and in situ data is good enough to suggest that Q_{latent} sources are achieving their accuracy goals. It was found that the satellite weekly τ_x, τ_y, and Q_{latent} exhibited the main known spatial and temporal characteristics at global and local scales. The local variability of the three surface parameters is well revealed by the satellite time series in tropical and in North Atlantic areas (with respect to buoy and ship data). The mean and rms difference between buoy and remotely sensed flux estimates are quite low.

For instance, in the Tropics, the bias values for wind stress and latent heat flux are 0.5×10^{-2} N m^{-2} and 7 W m^{-2}, respectively. The corresponding rms values are 1.5×10^{-2} N m^{-2} and 29 W m^{-2}. In the equatorial Pacific, the bias is -0.8×10^{-2} N m^{-2} and −23 W m^{-2} respectively (see Table 1) and does not vary much according to the Pacific areas (east, center, or west).

b. TAO buoy network

To objectively evaluate the various sensitivity simulations in the tropical Pacific, we used the temperature and current data of the TAO buoy network. The TAO buoys have been deployed since 1979, and the array has about 70 buoys. They are distributed in the tropical Pacific from 8°S to 9°N and from 135°E to 95°W. For this study, we use data from 16 buoys that provide sea

temperature measurements located at 5°S and 5°N and 147°E, 156°E, 170°W, 140°W and 110°W from the surface down to 500-m depth. Current data are available at two TAO buoy locations, 170°W–0° and 110°W–0° and from the surface down to 350-m depth. The parameters used here are monthly averages calculated from daily estimates.

c. Sea surface temperature analysis

Two SST products are used in this study. First we used daily optimally interpolated SST data calculated from the Reynolds and Smith (1994) weekly analysis available at the National Meteorological Center (National Centers for Environmental Prediction) from 1994 to 1998. The SST spatial resolution is 1° latitude and longitude on the global ocean. They are indicated as RS94. The second product is the Reynolds and Smith (1994) SST 1994–96 average seasonal cycle (indicated as RS94 hereafter).

d. OGCM

The OGCM used here is the Office of Ocean Resources Conservation and Assessment (ORCA) model (Delecluse et al. 1993) in its rigid lid version and in forced mode. This model is explained in detail in Madec et al. (1998) and has global coverage. The model grid resolution is 0.5° and 1.5° latitude and 2° longitude, with the smaller grid size at the equator and 31 vertical levels: 10 m for the first 150 m. For depth between 150 and 500 m the resolution varies between 20 and 150 m. The latter lies between 300 and 500 m for depth higher than 500 m. The time step is 1.5 h.

The vertical mixing is parameterized using the turbulent Kinetic energy equation (Blanke and Delecluse 1993). The lateral diffusion is the same as in Vialard et al. (2001). The sea ice is parameterized by a simple test on the sea surface temperature. This means that a constant heat flux is imposed in the presence of ice: −2 W m^{-2} in the Arctic and −4 W m^{-2} in the Antarctic.

e. Forced ocean experiments

To evaluate the contribution of the satellite wind stress (*ERS-1/-2*) and latent heat flux (multisatellites) in the oceanic circulation, three experiments have been performed. The first experiment is used as a reference experiment (EXP1) and is forced with daily ECMWF analysis fluxes from 1994 to 1999 (wind stress, latent, sensible and radiative heat fluxes, and freshwater fluxes). The net heat flux applied to the ocean surface is as follows:

$$Q_{\text{model}} = Q_O + K(\text{SST}_m - \text{SST}_O), \qquad (3)$$

where Q_O stands for the net budget provided as input for the model and given by

$$Q_O = Q_{\text{short}} + Q_{\text{long}} + Q_{\text{latent}} + Q_{\text{sensible}} \qquad (4)$$

and Q_{short}, Q_{long}, Q_{latent}, and Q_{sensible} are the net incoming shortwave radiation, net outgoing longwave radiation, latent heat flux, and sensible heat flux, respectively; SST_m is the model sea surface temperature, which is relaxed every 30 days toward SST_O; SST_O is the daily mean climatological sea surface temperature estimated from Reynolds and Smith (1994, RS94); and K is taken as a constant and is equal to -40 W m^{-2}/K. Even though K would be overestimated in some oceanic areas such as the tropical basins where the ocean–atmosphere interactions are highly sensitive (Oberhüber 1988; Barnett et al. 1991), its value is kept constant in order to avoid inconsistent SST estimates (Vialard et al. 2001). To reduce model errors related to the freshwater estimates (derived from ECMWF analysis), sea surface salinity (SSS) is relaxed toward Levitus climatology (Levitus 1998). However, throughout this paper the analysis of the forcing results will not focus on SSS. The initial state (spinup) of EXP1 is obtained after 10 yr of the model integration forced by the daily climatological fluxes for 1994–96 derived from ECMWF analysis.

To evaluate the impact of the satellite fluxes, a second experiment (EXP2) is forced with the same forcing fluxes of EXP1 but with the ECMWF latent heat fluxes replaced by daily satellite estimates computed by interpolation from the weekly fields during the period 1996–98. The initial conditions of EXP2 correspond to EXP1 state at 31 December 1995. A third experiment (EXP3) is performed using both the daily satellite wind stresses and satellite latent heat fluxes instead of the ECMWF estimates. The initial conditions of EXP3 are the same as those of EXP2.

To assess the impact of the weekly-to-daily interpolation methods, weekly wind stress computed from daily ECMWF analysis is interpolated to daily estimates and compared to the original ECMWF daily fields over the tropical Pacific. The mean difference of wind stress is very small (-0.08×10^{-2} N m^{-2}) and represents about 2% of the mean wind stress amplitude (Table 1), whereas the mean bias with the satellite wind stress is about 15%. An additional experiment was then carried out with this new daily ECMWF wind stress. The solutions from this experiment are very similar to EXP1, indicating that choosing daily or weekly ECMWF does not have a significant impact on the tropical Pacific dynamics in terms of monthly mean analysis of the model output.

3. Impact of satellite wind stress and latent heat flux

a. Comparison of mean forcing fluxes

The quality of the oceanic simulations should be related to the forcing function used in each experiment. Figure 1 presents the three years (1996–98) and zonal averages (between 30°S and 30°N) in the Pacific Ocean, of the zonal (Fig. 1a) and meridional (Fig. 1b) wind stress components, net heat flux (Fig. 1c), and net freshwater flux (Fig. 1d) applied to the model, net heat flux absorbed by the model (Fig. 1e), and the SST difference (Fig. 1f). We notice that latitudinal ECMWF wind stress (black line) is stronger than the satellite (red line) (Figs. 1a,b). An analysis of the seasonal variability of ECMWF and satellite wind stresses (figures not shown) indicates that both exhibit the same space variance patterns. However, the amplitude of the variability of the remotely sensed wind stress is almost everywhere weaker than the ECMWF estimates. Within the equatorial area, the differences during 1997 are less than those estimated during 1996 and 1998. Such different behavior is related to wind variability and to the bulk parameterization used to calculate wind stress from surface winds. Furthermore, it is found out that the difference is systematically significant for nearly all longitudes, with a maximum of about 0.2×10^{-2} N m^{-2} located in western and central Pacific equatorial area in 1996. Because of wind distribution over the tropical Pacific Ocean, zonal wind stress exhibits higher difference (Fig. 1a) than the meridional component (Fig. 1b).

Both differences between ECMWF and remotely sensed net flux estimates (Fig. 1c) and between evaporation and precipitation ($E - P$) estimates (Fig. 1d) are closely related to latent heat flux difference. The latter is probably due to the bulk parameterization used (Smith 1988) to estimate the exchange coefficient [Eq. (2)]. Indeed, previous studies (Renfrew et al. 2002; Bentamy et al. 2003) showed that the ECMWF exchange coefficient is overestimated compared to the Smith model (Smith 1988). We can notice that the net flux difference reaches a maximum of about 50 W m^{-2} in the subtropical area where surface winds are high. Furthermore, this difference varies in space and time. It is higher during 1996 and 1998, and in the western area, reaching 60 W m^{-2}, while in the central area it does not exceed 40 W m^{-2}.

b. Ocean responses

The results derived from the oceanic forcing experiments are first investigated through the absorbed surface net flux heat. The net flux absorbed is the sum of the nonpenetrative heat flux (includes sensible, latent,
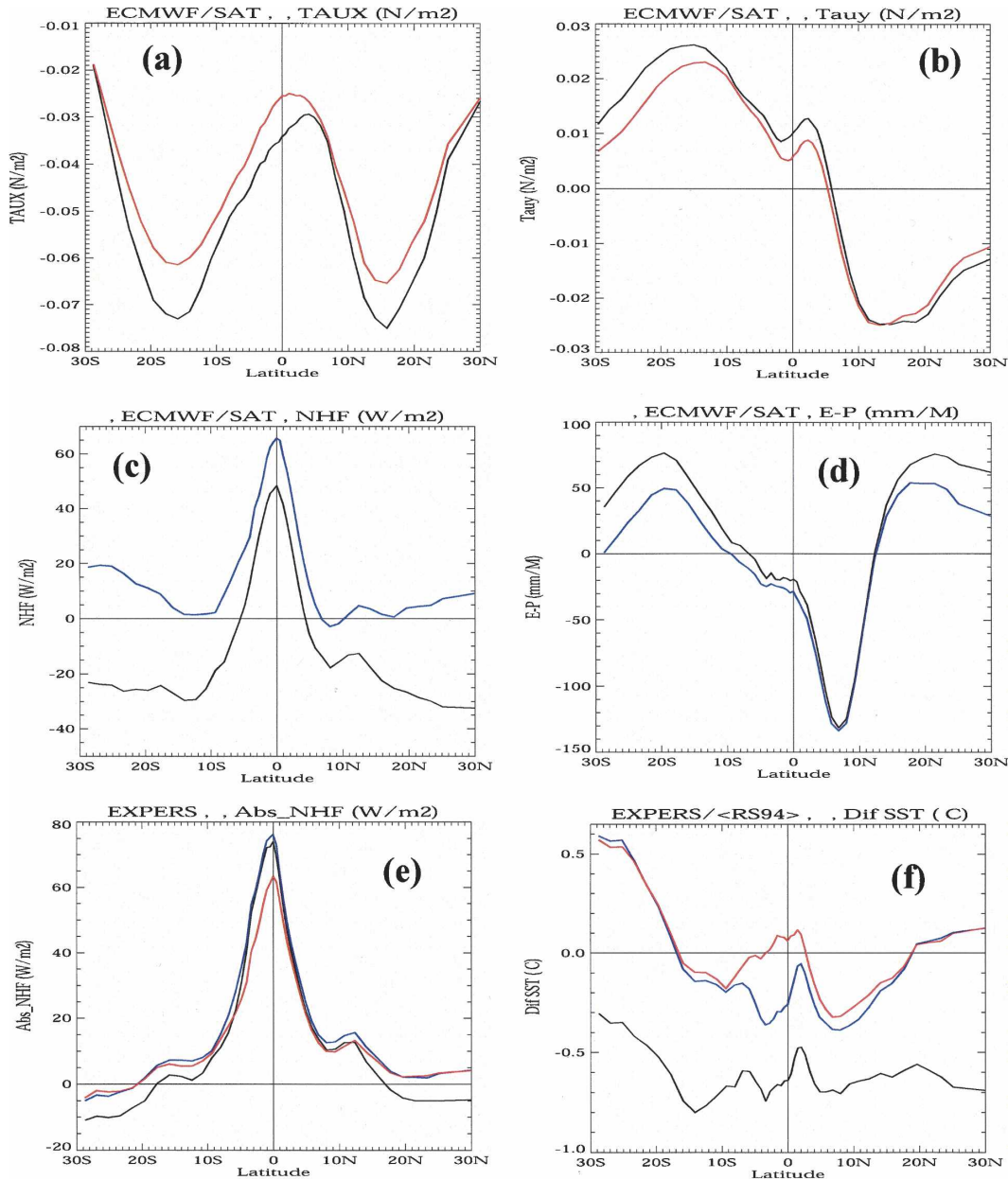
FIG. 1. Comparison of 3-yr means of relevant variables in the simulations: (a) zonal and (b) meridional wind stress from ECMWF analysis (black line) and *ERS-1/-2* (red line); (c) net heat flux and (d) net freshwater flux when all components are from the ECMWF analysis (black line) and when the latent heat flux is derived from satellite measurements (red and blue lines); (e) the absorbed heat flux of the three simulations and (f) the difference of their SST with the values of Reynolds and Smith (1994)RS94) for EXP1 (black), EXP2 (blue), and EXP3 (red).

and longwave heat fluxes) plus the penetrative solar heat flux, which depends of the fraction of solar flux heating that reaches the mixed layer depth (Jerlov 1968). The mixed layer depth is determined using the density criterion: the bottom of the first model level where density is higher than the sea surface density plus 0.05 kg m^{-3}. This criterion is often used in the tropical

simulations (Ayina and Servain 2003; Vialard et al. 2001). Figure 1e represents the zonally averaged absorbed heat fluxes derived from EXP1 (black color), EXP2 (blue color), and EXP3 (red color). The three simulations provide considerable absorption of heat occurring within 10°S and 10°N. However, EXP1 and EXP2 results are higher than EXP3. This difference in

response from one simulation to another is explained by the depth of the mixed layer, which depends on wind stress. Indeed, the heat absorbed by the mixed layer depends on the fraction of shortwave radiation that reaches the mixed layer depth. A deep mixed layer should capture the maximum amount of solar short-wave radiation, while a shallow layer should lose the solar radiation toward subsurface layers. In the case of EXP3, the ocean loses much heat toward subsurface layers at the equator due to a shallower mixed layer associated with the weaker remotely sensed wind stress. In the equatorial area the difference between absorbed fluxes derived from EXP1 and EXP2 is quite small. This is also related to the relaxation term (3) yielding to a significant reduction of heat differences. This means that the sea surface temperatures of EXP1 and EXP2 are underestimated.

The discrepancies between the simulations are first investigated through the comparisons of the zonal average of the differences between SST resulting from each experiment and RS94 SST estimates in Fig. 1f. This figure shows that the SST of EXP1 (black line) is smaller than RS94, which implies a strong relaxing term toward SST higher than 20 W m^{-2} between 20°S and 35°N. It was found that SST biases are larger in the west and the center of the basin, where they are about −1.0°C. In the eastern part of the basin, the SST derived from EXP1 is in general warmer than RS94, which is related to the weakness of the coastal up-welling in the model. When one replaces the ECMWF latent heat flux with the satellite estimates (EXP2: blue), these biases, from the relaxation term, are reduced and become lower than 10 W m^{-2} between 20°S and 35°N. This corresponds to a difference in SST of about −0.3°C. When both the satellite wind stress and latent heat flux are used (EXP3), SST differences are further reduced to about −0.2°C. This tends to show that the satellite latent heat flux has an important contribution to the simulation of SST in the tropical Pacific during this 3-yr period and especially in the subtropical regions, where it explains a departure from RS94 of about 0.5°C. The response of the ocean in EXP2 and EXP3 illustrates a low sensitivity of the tropical Pacific to *ERS-1/-2* winds compared to those of ECMWF. The impact of satellite wind stress is considerably lower than the impact of latent heat flux one (blue line). This is mainly related to the high correlation between satellite and ECMWF winds (Fig. 1). An exception is the area near the equator where weak *ERS-1/-2* is associated with a strong SST because of weak equatorial up-welling and thus is also associated with a cooling of the surface by the relaxation term (Fig. 1f). However, within 10°S and 10°N, the impact of remotely sensed

wind stress is significant. The observed cooling in EXP1 and EXP2 is consistent with the wind stress differences found in 1996 [see section 3c(2)] in western and central regions. The former explains the SST departure of −1.0°C for EXP1 and −0.5°C for EXP2. EXP3-derived SST exhibits a positive bias along the tropical Pacific Ocean.

Last, beyond ±20°, the behavior of the ocean in simulations EXP2 and EXP3 is different between the north and south areas. In the north (north of 20°N) the simulated temperatures are slightly warmer than RS94 estimates, whereas they are much warmer in the south (south of 20°S), which implies a strong relaxation term of about −25 W m^{-2} there.

c. Comparisons with buoy measurements

To enhance the comparisons between the three forcing experiments, their oceanic results are compared to measurements from TAO buoys moored in the tropical Pacific Ocean. The comparison analyses are focused on the mean and variability of sea temperature and current.

1) MEAN PATTERNS

Figures 2 and 3 shows the vertical profiles of the mean temperature (between 0- and 300-m depth) at TAO moorings located in the western (Figs. 2,b,c), central (Figs. 2d,e,f), and eastern regions (Figs. 3a,b,c) of the tropical Pacific. For comparison purposes, the vertical temperature values derived from the three simulations are interpolated to the TAO buoy locations and time averaged during the period 1996–98. The averaged buoy vertical profiles, indicated by the dashed line in Figs. 2 and 3, are calculated from seven buoys in the western and central areas and from two buoys in the eastern area. The black, blue, and red colors indicate the interpolated vertical profiles derived from EXP1, EXP2, and EXP3, respectively. In general there is a good agreement between buoy and model estimates, especially between 0- and 100-m depth. The thermocline in the model is at nearly the same depth as in the buoy data. However, it appears that the model is too diffuse, letting heat escape toward the subthermocline layers and producing subsurface water that is too warm compared to TAO. This problem is slightly reduced consistent with the results of Menkes et al. (1998). Even though EXP3 provides some improvement, its derived vertical temperature remains warmer than buoy estimates. This could be related to the parameterization of the vertical mixing used in the model (Blanke and Delecluse 1993). In the west and between the surface and 80 m, the temperatures of EXP2 and
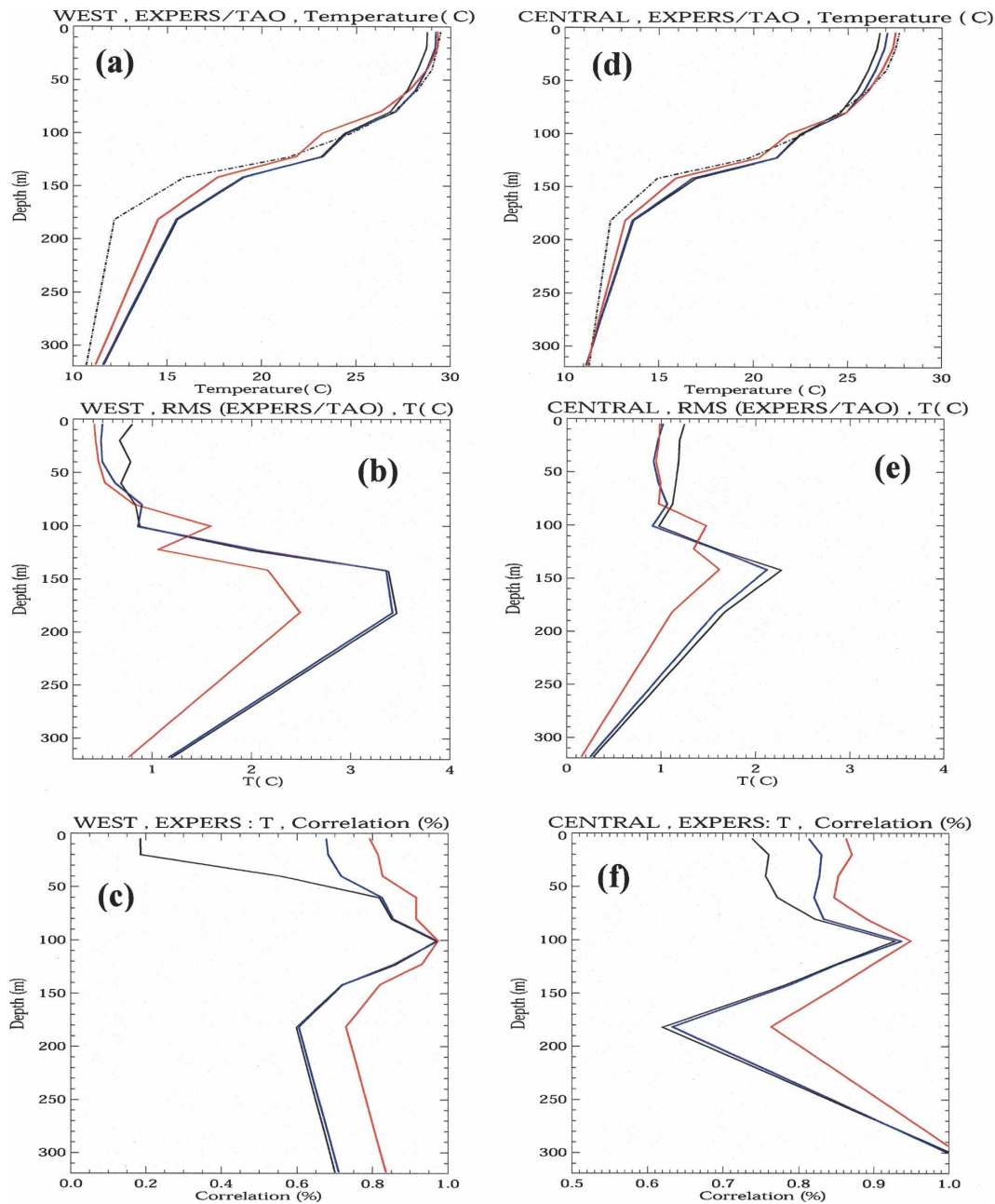
FIG. 2. Comparison between simulations and TAO, averaged over 1996–98: (a) the vertical temperature structure, (b) rms difference of temperature, (c) correlation of the temperature, at west Pacific (5°–5°S, 156°E–180°). (d), (e), (f) Same as in (a)–(c) but for central Pacific (5°S–5°N, 170°–140°W). The black dotted line is TAO, the black solid line is EXP1, the blue line is EXP2, and the red line is EXP3.

EXP3 are closer to the observations (Fig. 2). The thermocline is reasonably represented and it is located at 120-m depth, as illustrated by the standard deviation behaviors (Fig. 2a).

In the eastern basin the thermocline is located around 80 m (Fig. 2b). The rms difference and correlation coefficients are worse compared to the parameters calculated in the western area. The rms values are about 2.0°C at the surface in the east versus 1.0°C in the west and the center. The surface correlations are lower and about 70% in the three experiments. This deterioration may be related to the relaxing term forcing SST toward climatology, whereas during this period (1997–98) one of the warmest temperature anomalies of the
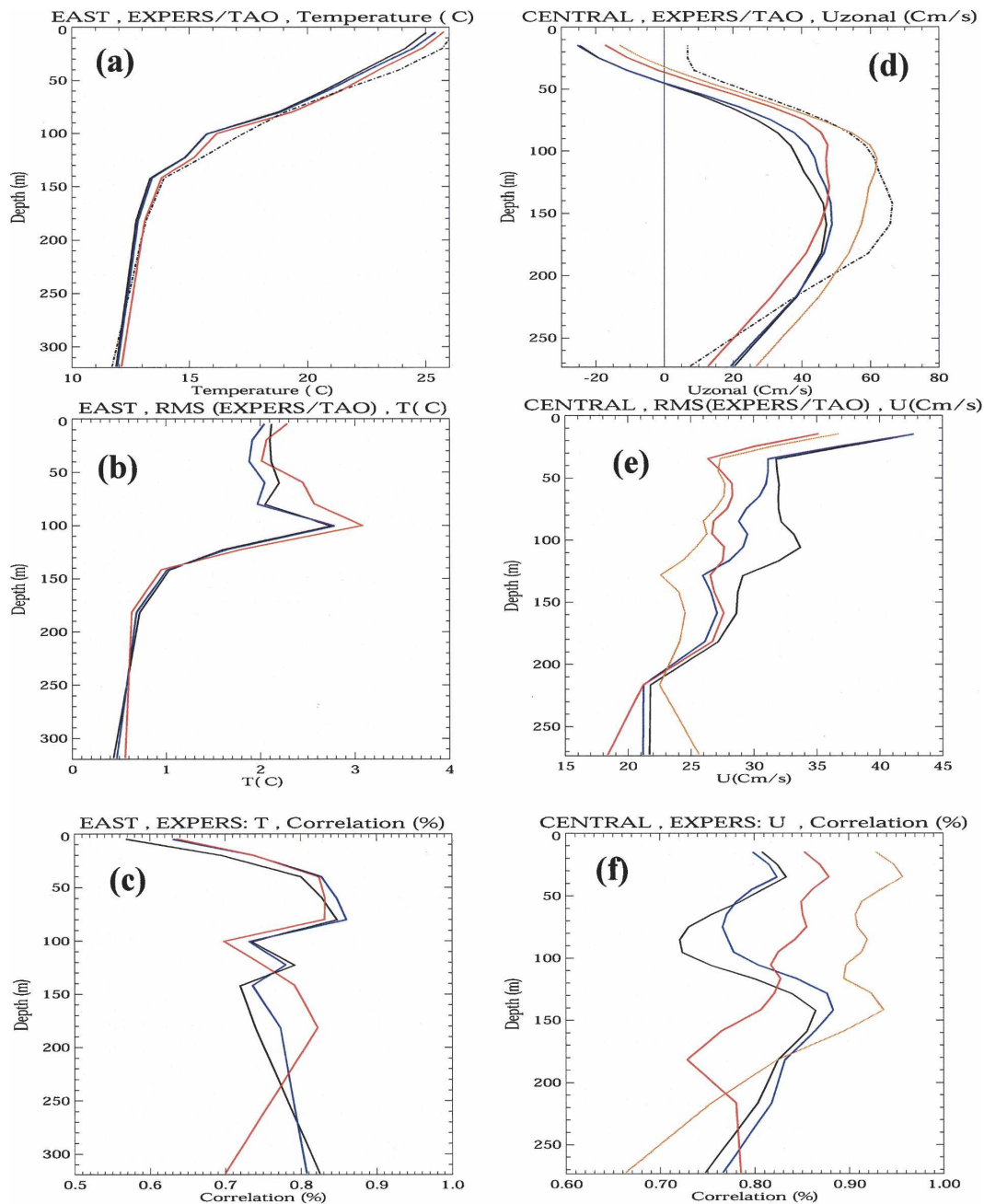
FIG. 3. Same as in Fig. 2 but for (a)–(c) at east Pacific (5°–5°S, 140°–110°W) and (d)–(f) for the zonal current at central Pacific (5°S–5°N, 170°–140°W). The orange line is the simulation with the satellite wind stress increased by 50%.

last 20 yr occurred (Wang and McPhaden 2001). The collocation procedure used to compare buoys and model results may have some impact on the difference between the two sources. For instance, in this region the surface winds estimated from the scatterometer are underestimated according to buoy estimates (Dickinson et al. 2001; Bentamy et al. 2002b). Such impact is more pronounced in EXP3 mainly because of weaker

remotely sensed wind stress and the corresponding bulk parameterization.

The averaged zonal currents are illustrated in Figs. 3d,e,f . The in situ current data are derived from TAO buoys located at the equator at 170°W. The averaged simulation currents are estimated from the nearest grid points from buoy location and from depth levels where buoy currents are available (the first level is located at

15-m depth). Figure 3d shows that the model represents in a satisfactory way the vertical structure of current in the center basin, and the same is true for the eastern basin (figure not shown). The main differences are found in the first 50 m, where the differences between various simulations and the observations are generally higher than 40 cm s^{-1}. This is due to the model poor representation of the inversion of the southern equatorial current (SEC) during 1996 and 1998, especially in the eastern part of the basin (see Fig. 6). The model tends to underestimate the under current in the eastern area with a mean value about of 60 cm s^{-1}, while the TAO buoy indicates 90 cm s^{-1}.

On the other hand, in the central area the vertical structure of the current is sensitive to the satellite fluxes. EXP3 indicates a slight improvement compared to EXP1 and EXP2. The correlations (rms difference) characterizing the comparison between buoy and EXP3 are generally higher (lower) than 80% (25 cm s^{-1}) in the first 150 m. One can also notice a slight sensitivity of the currents to the satellite latent heat flux. This sensitivity is found between 50 and 150 m where the rms (correlations) of EXP2 are lower (higher) than those estimated from buoy and EXP1 comparisons. This may be related to the pressure gradient change, which is deteriorated by the diffusion of heat toward the subsurface.

2) VARIABILITY

To further analyze the quality of the simulations, the spatial and temporal variability of temperature and current are investigated through comparisons with buoy measurements and/or Reynolds and Smith (1994). Both Figs. 4 and 5 represent the time evolution of the averaged water temperature at 50-m depth and of some diagnostic parameters calculated over oceanic areas in the western and central tropical Pacific, respectively. It shows that in 1996, the temperature in the mixing layer is high in the western part of the basin (with values exceeding 29.5°C), but it is low in the central region, where it varies between 24° and 26°C. Early in 1997, the temperature drops in the western part of the basin until about 28°C in February 1998. The temperature increases quickly on the other hand in the central part of the basin to reach its maximum (29°C) at the end of 1997. The interannual anomalies of temperature in these areas are about 4°C (Wang and McPhaden 2001). Then in April 1998, the temperature is heated again in the western tropical Pacific reaching 29.5°C and falls quickly in the eastern (22°C) and in the central (26°C) regions.

The El Niño events of 1997–98 and La Niña events of 1998–99 are clearly depicted through these time series.

These events are known and have been described by many authors (see, e.g., McPhaden 1999; Wang and Weisberg 2000; Wang and McPhaden 2001). In spite of the fact that the model was relaxed toward the seasonal climatology of RS94, it restores features of these events quite well during the period 1996–98. The warming during 1996 and the cooling during 1997–98 in the west as well as the warming during 1997 in the center of the basin are all well retrieved. Table 2 summarizes the interannual variation and correlations between RS94 and the simulated interannual anomalies of the mixing layer temperatures in the western and central areas. Statistics calculated in the eastern area are provided too. The best statistical parameters are found for RS94 and EXP3 comparisons. The latter provides interannual anomaly features that are very similar to the observations, especially in the western and central areas where the correlation exceeds 80% and the variance is comparable to RS94. The impact of the latent heat flux is mainly significant in the western and central basins, where the correlation increases from nearly 70%–86%. Again in the eastern area the statistics are slightly poorer than in the two previous regions.

To further analyze the physical mechanisms involved in the model response to the impact of satellite turbulent fluxes, the temporal features of the main forcing terms controlling the temperature in the mixed layer are investigated. Figures 4a and 5a show the averaged time series of temperature at 50-m depth; Figs. 4b and 5b, zonal wind stress; Figs. 4c and 5c, isotherm 20°C depth (Z20); Figs. 4d and 5d, latent heat flux; Figs. 4e and 5e, relaxing heat flux (RHF); and Figs. 4f and 5f, and applied fluxes at surface (net heat flux and relaxation flux term), calculated at buoy locations in the western and central areas, respectively. In 1996, the ECMWF zonal wind stress exhibits high values over the whole equatorial Pacific basin, with a maximum in the central region. In response, the western gradient of Z20 is quite evident. The western and central thermocline is found at 200 and 160 m, respectively. The interannual anomalies of the tendency term of the mixing layer temperature indicate (Table 3) a strong activity of vertical processes (-1.0°C month^{-1} in the central Pacific) but also meridional advection (-0.15°C month^{-1} in the western Pacific), yielding to a strong cooling of the surface in these areas. In parallel, the strong cooling of the surface (Fig. 4d) by ECMWF evaporation leads to a weak mixed layer temperature in EXP1 lower than the RS94 climatology. Therefore, the relaxing term tends to erase such departures from climatology by applying a significant quantity of heat about 50 W m^{-2} in the west and 100 W m^{-2} in the center (Fig. 4e). Figures 4a and 5 indicate that the use of remotely sensed heat flux
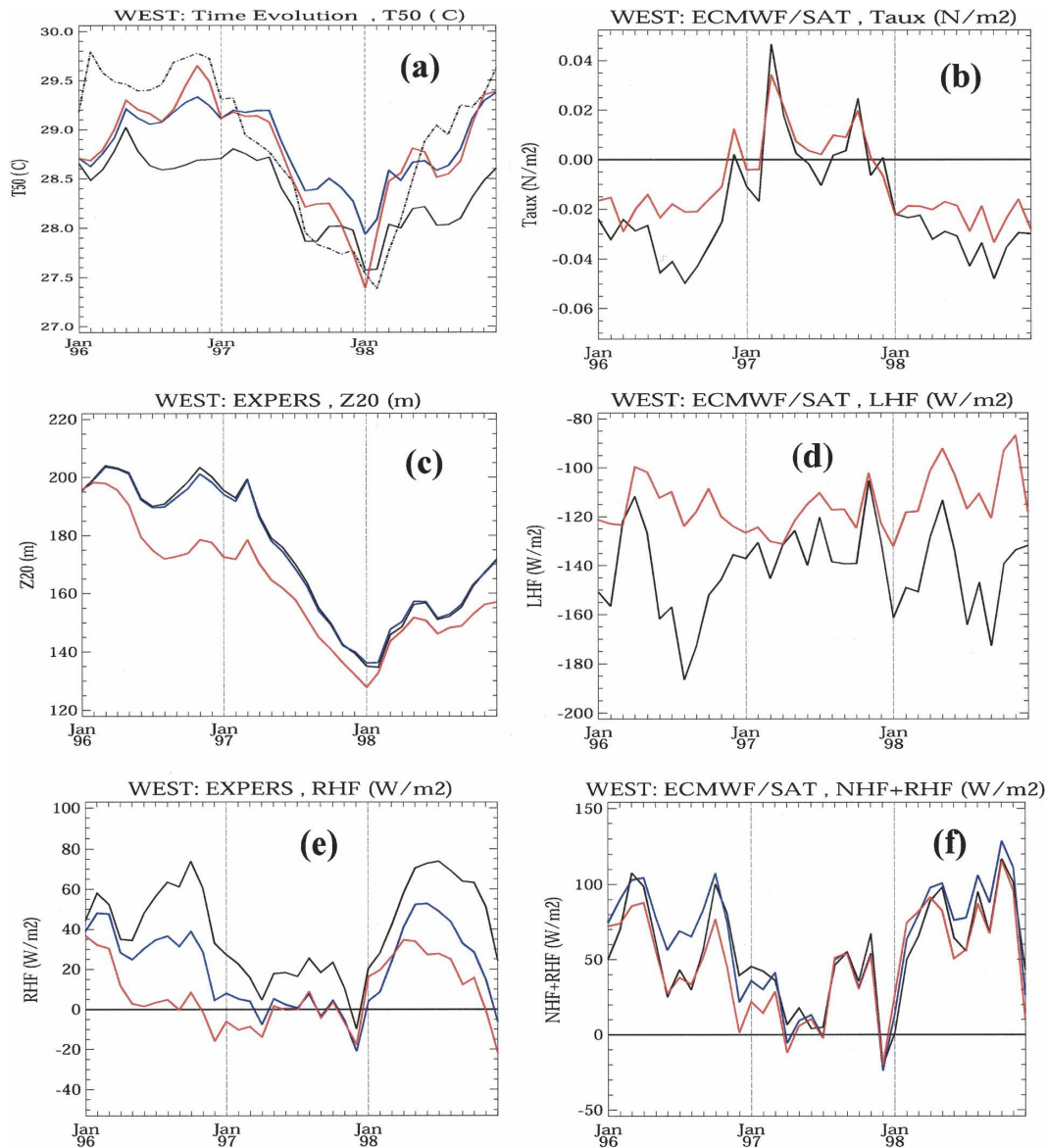
FIG. 4. January 1996 to December 1998 evolution in the western tropical Pacific: (a) 50-m mean temperature, (b) ECMWF (black) and satellite (red) zonal wind stress, (c) 20°C isotherm depth (m), (d) ECWMF (black) and satellite (red) LHF, (e) RHF, and (f) the net heat flux applied to the ocean surface (NHF + RHF). In (a) the dotted line represents TAO temperature. In (a), (c), (e), and (f), the black line indicates EXP1, the blue line EXP2, and the red line EXP3.

within EXP2 leads to less cooling of the 50-m temperature (Fig. 4a and Fig. 5a) and, as expected, to lower relaxing heat flux than in EXP1 (Fig. 3e and Fig. 5e). However, the difference between the vertical Z20 derived from EXP1 and EXP2 is quite negligible. The latter is more significant when satellite wind stress and latent heat flux are used together (EXP3), implying a low depth of Z20. The temperature increase, compared to the two previous experiments, is a result of the vertical processes and low satellite evaporation. The relax-

ation flux impact is quite small, and its values are about 5 W m^{-2} in the western and 20 W m^{-2} in the central regions.

In the western area the wind stress weakens by the end of 1996 and exhibits high easterly winds early in 1997. The oceanic response indicates that Z20 level reaches its minimum late in 1997 in the western as well as in the central regions. The surface currents (Fig. 6) are reversed and leading to advection of hot water from the warm pool toward the east. The temperature in-
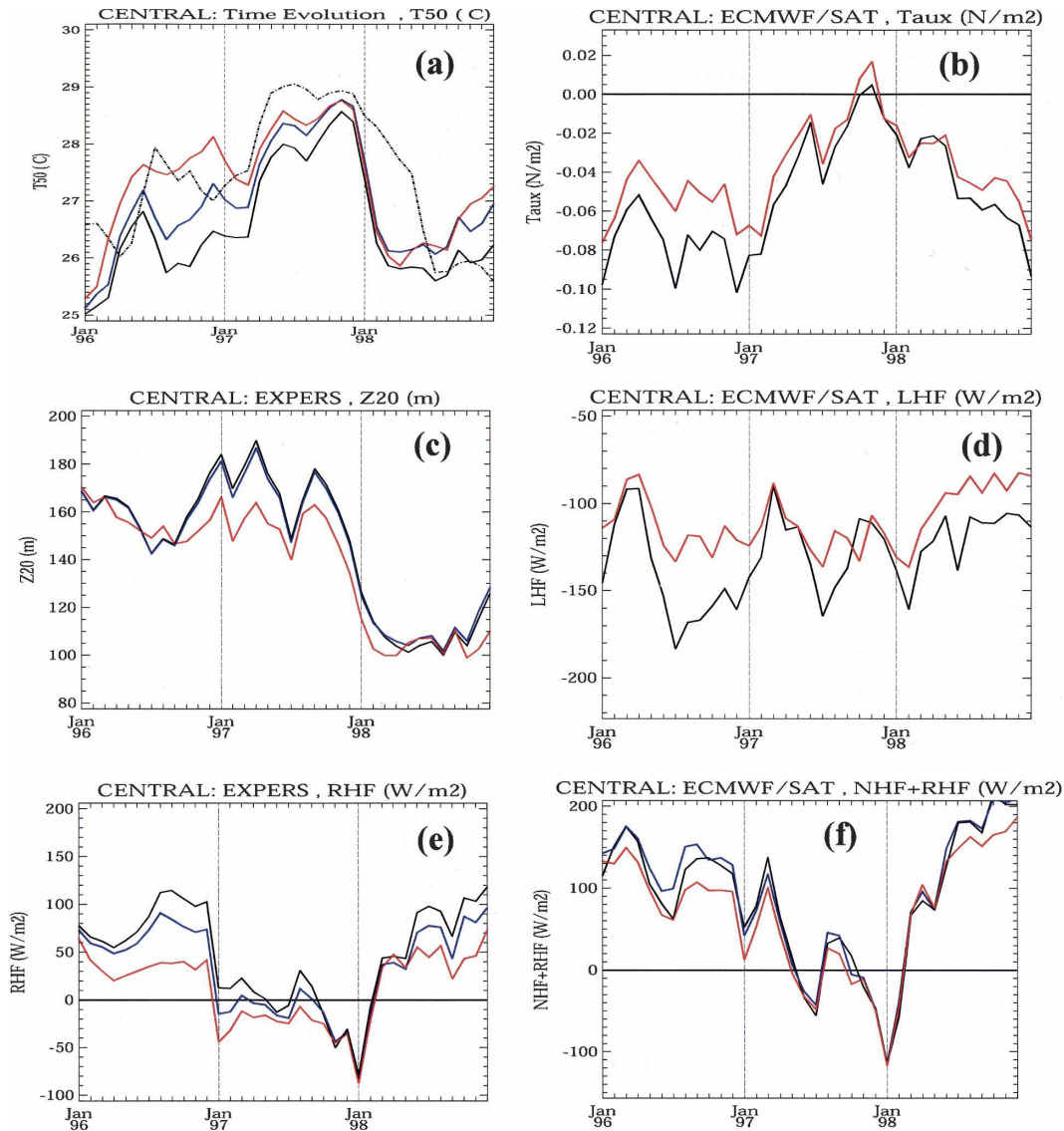
FIG. 5. Same as in Fig. 4, but for the central tropical Pacific.

creases from about 27° to 28.5°C (EXP3) in the central zone (Fig. 5a). However, the three simulations exhibit smaller temperature differences during 1997 than during 1996. This is in connection with the lower differences between ECMWF and satellite wind stress and latent heat fluxes, especially in the central area. During 1997 the relaxation heat flux is slightly strong (see Figs. 4f and 5f). The vertical processes were also very weak ($+0.20°C$ month^{-1}). Although the model retrieves the temperature increase of 1997–98 well (especially in the central area), it does not restore the drop of the temperature 4 months before the observations. Both Figs. 4e and 5e suggest that the relaxing heat flux tends to minimize the temperature increase for this period. In-

deed, at the end of 1997, the relaxing flux inflects on the ocean a negative heat of about -90 W m^{-2} in the central basin, which in turn constrains the model to set out toward the temperature of the season (cooling).

In addition, it is also noted that in the three simulations Z20 rises to the surface, whereas the SST is hot in the east and in the center of the basin. These results are in good agreement with Wang and McPhaden (2001), even though the rising rate is not weak in the center and especially in the east areas. The coupling between the strong winds with Z20 close to the surface combined with a strongly relaxing negative flux are the main causes explaining the early cooling of the surface in the three experiments.

TABLE 2. Statistical parameters [interannual std dev (°C)/ correlations (%)] characterizing the comparisons between simulations and RS94 temperature in the western (160°E–180°), central (170°–140°W), and eastern (130°–110°W) Pacific, between 2°S and 2°N.

Variance/correlation	West	Central	East
RS94	0.90°C	2.1°C	2.4°C
EXP1	0.78°C/0.68	1.2°C/0.77	1.3°C/0.65
EXP2	0.81°C/0.86	1.4°C/0.80	1.5°C/0.69
EXP3	0.91°C/0.95	1.9°C/0.85	2.0°C/0.75

4. Summary and conclusions

Forcing an oceanic general circulation model with surface fluxes and comparing the results of the simulations with observations is a valuable method to evaluate the quality of the fluxes. The findings of this study support the assumption of several operational oceanic programs (e.g., the European Mercator, MERSEA, and MFSTEP) that using satellite fluxes to complement or substitute surface atmospheric analyses (like ECMWF) can improve their simulations of the thermal structure and the upper-ocean circulation. In this paper, we used the ORCA model of the Laboratoire d'Océanographie

TABLE 3. Estimates of total zonal and meridional advection, forcing, and subsurface tendency contribution to the SST budget at the (a) west and (b) central Pacific. The mean value is the 1994–96 average, and the others two values respectively correspond to the interannual anomalies in 1996 and the El Niño 1997–98 period.

| (a) West Pacific				
Tendency (°C month⁻¹)	Zonal	Meridional	Forcing	Subsurface
Mean value	−0.37	0.04	0.69	−0.31
Anomalies EXP1	0.10	−0.15	0.40	−0.15
	0.50	0.00	−0.80	0.20
EXP2	0.01	−0.15	0.50	−0.25
	0.50	0.00	−0.60	0.30
EXP3	0.30	−0.10	0.02	0.10
	0.50	−0.01	−0.60	0.30
(b) Central Pacific				
Tendency (°C months⁻¹)	Zonal	Meridional	Forcing	Subsurface
Mean value	−0.13	0.10	1.66	−1.65
Anomalies EXP1	0.20	−0.10	0.50	−1.00
	0.30	0.20	−1.20	1.20
EXP2	0.30	−0.10	0.60	−1.10
	0.30	0.22	−1.25	1.20
EXP3	0.10	−0.20	−0.05	0.50
	0.30	0.18	−1.25	1.25
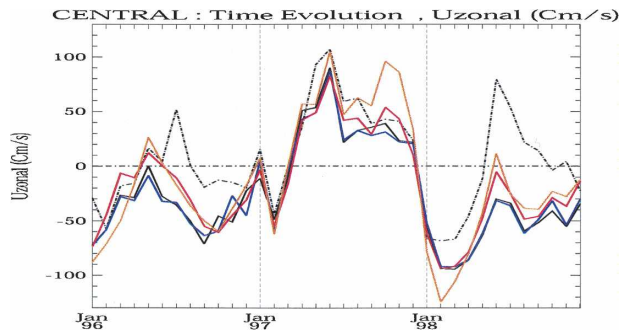
FIG. 6. January 1996 to December 1998 evolution of zonal current in the central tropical Pacific: the dotted line represents TAO, the black line EXP1, the blue line EXP2, and the red line EXP3. The orange line denotes times when the satellite wind stress is increased by 50%.

Dynamique et de Climatologie (LODYC) to evaluate, through the response of the ocean forced by satellite wind stress and latent heat flux (evaporation) as well as ECMWF atmospheric analyses, the quality of satellite turbulent fluxes.

We focused on the response of the equatorial Pacific Ocean during the period 1996–98. The oceanic responses (temperature and current in the first 500 m) are compared with in situ data derived from the TAO buoy and with Reynolds and Smith (1994) SST time series. We described the temperature and ocean current responses of the upper tropical Pacific Ocean during 1996–98. The results were compared with observations from the TAO buoy network and the SST of Reynolds and Smith (1994).

We showed that the ORCA model is able to reproduce the mean structures and the interannual evolution of the main variables in the equatorial Pacific, from the surface through 500-m depth during the period 1996–98. The model exhibits a good agreement with observations and with previously published studies. For instance the mean values of the total zonal and meridional advection, forcing, and subsurface tendency contribution to the SST budget match results obtained by Wang and McPhaden (1999) and by Vialard et al. (2001). Similar good agreement is found for the interannual anomalies of these terms during the 1996–98 period. Furthermore, the implied zonal advection in El Niño is in agreement with the conclusions of Picaut et al. (2001).

The relaxation term of SST that represents the feedback between the ocean and atmosphere in a forced simulation where atmosphere is prescribed shows clearly that the forced ocean with satellite turbulent fluxes (the latent heat flux and particularly when they are associated winds *ERS-1/-2*) provides better results,

when compared to observation, than ECMWF forcing experiments. The sensitivity simulations show that the experiments forced only by satellite turbulent fluxes [wind stress and latent heat flux (EXP3)] reveal the closest features with respect to observations in terms of mean as well as in terms of interannual variability. This study also indicates that on average the wind stress field modifies the averaged mean vertical structure of temperature and currents, and thus contributes to enhancing the issue related to the diffusion excess meets oceanic model as ORCA (as in Menkes et al. 1998).

In spite of these good agreements, several drawbacks are found. For example, the temperatures and then their anomalies in the central and eastern parts of the tropical Pacific are weaker during the 1997–98 El Niño. This result is connected to the relaxation term constraining the model to the seasonal temperature. The end of the 1997–98 El Niño four months earlier in the model compared to the observations is also related to the relaxation term. Some weakness of the model temperature can also be due to the excess evaporations and weak solar fluxes in the ECMWF analysis. Indeed, the net heat flux is dominated by the compensation between these two fluxes, and therefore an unspecified error in one of them leads to a departure of the oceanic response compared to the observations. This study shows that the relaxation term balances the weakness of the model and of the exchanged surface fluxes. Indeed, in the eastern equatorial Pacific, the thermal structure of the upper ocean forced by the winds and latent heat flux corresponds very well with those from TAO. In the west, the biases of SST with respect to TAO are almost 5 times larger when the ocean is forced by ECMWF turbulent fluxes. These results underscore the importance of forcing oceanic general circulation models with satellites turbulent fluxes. They also demonstrate that it is desirable to use a wind stress that is consistent with the latent and sensible heat fluxes. We plan to continue this work of evaluation of satellite fluxes by testing the new wind products from Quik-SCAT and their associated heat fluxes.

REFERENCES

Ayina, L.-H., and J. Servain, 2003: Spatio-temporal evolution of the low frequency climate variability in the tropical Atlantic. *Interhemispheric Water Exchange in the Atlantic Ocean,* G. J. Goni and P. M. Rizzoli, Eds., Oceanography Series, Vol. 68, Elsevier, 475–495.

Barnett, T. P., M. Latif, M. Kirf, and E. Roeckner, 1991: On ENSO physics. *J. Climate,* **4,** 487–514.

Bentamy, A., P. Queffeulou, Y. Quilfen, and K. Katsaros, 1999: Ocean surface wind fields estimated from satellite active and passive microwave instruments. *IEEE Trans. Geosci. Remote Sens.,* **37,** 2469–2486.

——, K. B. Katsaros, M. Alberto, W. M. Drennan, and E. B. Forde, 2002a: Daily surface wind fields produced by merged satellite data. *Gas Transfer at Water Surfaces, Geophys. Monogr.,* Vol. 127, Amer. Geophys. Union, 343–349.

——, Y. Quilfen, and P. Flament, 2002b: Scatterometer wind fields—A new release over the decade 1991–2001. *Can. J. Remote Sens.,* **28,** 431–449.

——, K. B. Katsaros, M. Alberto, W. M. Drennan, E. B. Forde, and H. Roquet, 2003: Satellite estimates of wind speed and latent heat flux over the global oceans. *J. Climate,* **16,** 637–656.

Blanke, B., and P. Delecluse, 1993: Variability of the tropical Atlantic Ocean simulated by a general circulation model with two different mixed layer physics. *J. Phys. Oceanogr.,* **23,** 1363–1388.

——, C. Roy, P. Penven, S. Speich, J. McWilliams, and G. Nelson, 2002: Linking wind and upwelling interannual variability in a regional model of the southern Benguela. *Geophys. Res. Lett.,* **29,** 2188, doi:10.1029/2002GL015718.

——, S. Speich, A. Bentamy, C. Roy, and B. Sow, 2005: Modeling the structure and variability of the Southern Benguela upwelling using QuikSCAT wind forcing. *J. Geophys. Res.,* **110,** C07018, doi:10.1029/2004JC002529.

Delecluse, P., G. Madec, M. Imbard, and C. Lévy, 1993: OPA version 7 ocean general circulation model, reference manual. Rapp. Interne LODYC 93/05, Laboratoire d'Océanographie Dynamique et de Climat, Paris, France, 111 pp.

Dickinson, S., K. A. Kelly, M. J. Caruso, and M. J. McPhaden, 2001: Comparisons between the TAO buoy and NASA scatterometer wind vectors. *J. Atmos. Oceanic Technol.,* **18,** 799–806.

Grima, N., A. Bentamy, P. Delecluse, K. Katsaros, C. Levy, and Y. Quilfen, 1999: Sensitivity of an Oceanic general circulation model forced by satellite wind stress fields. *J. Geophys. Res.,* **104** (C4), 7967–7989.

Jerlov, N. G., 1968: *Optical Oceanography.* Oceanography Series, Vol. 5, Elsevier, 194 pp.

Levitus, S., 1998: *World Ocean Atlas.* NOAA–CIRES Climate Diagnostics Center. [Available online at http://www.nodc.data.gov.]

Liu, W. T., and P. P. Niiler, 1984: Determination of monthly mean humidity in the atmospheric surface layer over oceans from satellite data. *J. Phys. Oceanogr.,* **14,** 1451–1457.

Madec, G., P. Delecluse, M. Imbard, and C. Lévy, 1998: OPA 8.1 ocean general circulation model, reference manual. Notes du pôle de modélisation 11, Institut Pierre Simon Laplace, 91 pp.

McPhaden, M. J., 1999: Genesis and evolution of the 1997–98 El Niño. *Science,* **283,** 950–954.

Menkes, C., and Coauthors, 1998: Impact of TAO vs. ERS wind stress onto simulations of the tropical Pacific Ocean during

the 1993–1998 period by the OPA OGCM. EuroCLIVAR Workshop Rep. 13, 46–48.

Mestas-Nuñez, A. M., A. Bentamy, and K. B. Katsaros, 2006: Seasonal and El Niño variability in weekly satellite evaporation over the global ocean during 1996–98. *J. Climate,* **19,** 2025–2035.

Oberhüber, J. M., 1988: An Atlas based on the COADS data set: The budgets of heat, buoyancy and turbulent kinetic energy at the surface of the global ocean. Rep. 15, Max-Planck-Institut für Meterologie, 20 pp.

Picaut, J., M. Ioulalen, T. Delcroix, F. Masia, R. Murtugudde, and J. Vialard, 2001: Displacements of an oceanic zone of convergence on the eastern edge of the Pacific warm pool: Consequences for ENSO and biogeochemical phenomena. *J. Geophys. Res.,* **106,** 2363–2386.

——, E. Hackert, A. J. Busalacchi, R. Murtugudde, and G. S. E. Lagerloef, 2002: Mechanisms of the 1997–1998 El Niño–La Niña, as inferred from space-based observations. *J. Geophys. Res.,* **107,** 3037, doi:10.1029/2001JC000850.

Renfrew, I. A., G. W. K. Moore, P. S. Guest, and K. Bumke, 2002: A comparison of surface-layer and surface turbulent-flux observations over the Labrador Sea with ECMWF analyses and NCEP reanalyses. *J. Phys. Oceanogr.,* **32,** 383–400.

Reynolds, R. W., and T. M. Smith, 1994: Improved global sea surface temperature analyses using optimum interpolation. *J. Climate,* **7,** 929–948.

Schulz, J., P. Schlüssel, and H. Grassl, 1993: Water vapour in the atmospheric boundary layer over oceans from SSM/I measurements. *Int. J. Remote Sens.,* **14,** 2773–2789.

——, J. Meywerk, S. Wald, and P. Schlüssel, 1997: Evaluation of satellite-derived latent heat fluxes. *J. Climate,* **10,** 2782–2795.

Smith, S. D., 1988: Coefficients for sea surface wind stress, heat flux, and wind profiles as a function of wind speed and temperature. *J. Geophys. Res.,* **93,** 15 467–15 472.

Vialard, J., C. Menkes, J.-P. Boulanger, P. Delecluse, E. Guilyardi, M. J. McPhaden, and G. Madec, 2001: A model study of oceanic mechanisms affecting equatorial Pacific sea surface temperature during the 1997–98 El Niño. *J. Phys. Oceanogr.,* **31,** 1649–1675.

Wang, C., and R. H. Weisberg, 2000: The 1997–98 El Niño evolution relative to previous El Niño events. *J. Climate,* **13,** 488–501.

Wang, W., and M. J. McPhaden, 1999: The surface layer heat balance in the equatorial Pacific Ocean. Part I: Mean seasonal cycle. *J. Phys. Oceanogr.,* **29,** 1812–1831.

——, and ——, 2001: Surface layer temperature balance in the equatorial Pacific during the 1997–98 El Niño and 1998–99 La Niña. *J. Climate,* **14,** 3393–3407.